Progress In Electromagnetics Research, Vol. 139, 407–422, 2013

DOMAIN DECOMPOSITION FE-BI-MLFMA METHOD FOR SCATTERING BY 3D INHOMOGENEOUS OBJECTS

Hong-Wei Gao, Ming-Lin Yang, and Xin-Qing Sheng*

Center for Electromagnetic Simulation, School of Information and Electronics, Beijing Institute of Technology, Beijing 100081, China

Abstract—The hybrid finite element-boundary integral-multilevel fast multipole algorithm (FE-BI-MLFMA) is a powerful method for calculating scattering by inhomogeneous objects. However, the conventional FE-BI-MLFMA often suffers from iterative convergence problems. A non-overlapping domain decomposition method (DDM) is applied to FE-BI-MLFMA to speed up the iterative convergence. Furthermore, a preconditioner based on absorbing boundary condition and symmetric successive over relaxation (ABC-SSOR) is constructed to further accelerate convergence of the DDM-FE-BI-MLFMA. Numerical experiments demonstrate the efficiency of the proposed preconditioned DDM-FE-BI-MLFMA.

1. INTRODUCTION

The hybrid finite element-boundary integral (FE-BI) method is proved to be a general and accurate numerical method for electromagnetic problems [1–4]. The multilevel fast multipole algorithm is a powerful tool for accelerating the matrix-vector multiplication and it is shown to have ability to solve electrically large and complex problems [5–7]. Through employing the multilevel fast multipole algorithm (MLFMA), the capability of FE-BI has been improved greatly [8]. Since BI results in a full matrix equation, the final matrix of FE-BI is a locally full matrix. It is difficult to solve this type of matrix efficiently, especially for the case of electrically large problems. When the FE-BI matrix is directly solved by iterative solvers, the convergence is very slow and sometimes it is even impossible to achieve. Then, two methods are

Received 31 March 2013, Accepted 26 April 2013, Scheduled 1 May 2013

* Corresponding author: Xin-Qing Sheng (xsheng@bit.edu.cn).

applied to improve the convergence of conventional FE-BI-MLFMA. One is to construct a preconditioner resembling the sparse FE matrix through replacing the boundary integral equation with the first-order absorbing boundary condition (ABC) [9]. Numerical experiments have demonstrated the fast convergence of solving FE-BI matrix adopting ABC preconditioner. The other one is to decompose the FE-BI matrix into the FE sparse matrix and the BI dense matrix, and handle the FE matrix by ILU factorization method independently [10, 11]. Although the above two methods can accelerate the convergence effectively, solving the inverse of a sparse matrix required in each method consumes large memory. This bottleneck limits the application of FE-BI-MLFMA in solving electrically large problems.

Domain Decomposition Method (DDM) has been recognized as an important measure for designing efficiently computational algorithms [12–16]. Recently, a non-overlapping finite element domain decomposition method has been applied successfully in electromagnetic scattering and radiation problems [17–24]. Numerical experiments demonstrate the efficient performance of DDM, especially for periodic structures. In DDM, the whole computational domain is first decomposed into several sub-domains, and boundary condition ensuring field continuity is employed at sub-domain interfaces. Each sub-domain is solved independently. Then the adjacent sub-domains are coupled by boundary condition at interfaces and the unique solution for the whole computational domain is obtained consequently. Because the original problem is torn into several sub-domain problems, DDM enables the analysis of very electrically large problems using existing computing resources.

In order to improve the convergence of the conventional FE-BI-MLFMA and save the computer memory, a non-overlapping domain decomposition method presented in [19, 20] is applied to FE-BI-MLFMA effectively. Additionally, a novel mixed absorbing boundary condition and block symmetry successive over relaxation (ABC-SSOR) preconditioner is proposed to further accelerate the convergence. The proposed method is successfully used for calculating scattering by 3D inhomogeneous objects.

The rest of the paper is organized as follows: Firstly, the formulation of DDM-FE-BI-MLFMA and the derivation of ABC-SSOR preconditioner are detailed in the next section. Then, numerical experiments are performed to investigate this hybrid method. Finally, conclusions are drawn.

2. FORMULATION

2.1. Domain Decomposition FE-BI-MLFMA Method

Consider scattering by an inhomogeneous object, whose surface is denoted as S. According to the conventional FE-BI-MLFMA [8], the computational domain is directly divided into interior domain and exterior boundary by S. The interior domain is denoted as V. The interior field is formulated into an equivalent variational problem (1) according to electromagnetic vector wave equation.

$$F(\mathbf{E}) = \frac{1}{2}\int_V \left[(\nabla\times\mathbf{E})\cdot\left([\mu_r]^{-1}\nabla\times\mathbf{E}\right) - k_0^2\left[\varepsilon_r\right]\mathbf{E}\cdot\mathbf{E}\right]dv + jk_0\int_S \left(\mathbf{E}\times\bar{\mathbf{H}}\right)\cdot\hat{n}ds \quad (1)$$

Here, $\bar{\mathbf{H}} = Z_0\mathbf{H}$, with $\mathbf{E}$ and $\mathbf{H}$ denoting the unknown electric field and magnetic field, respectively. In addition, Z_0 is the free-space impedance and k_0 is the free-space wave number. $\hat{n}$ denotes the outward unit vector normal to S. The field on the exterior surface is usually formulated into the following combined field integral equation (CFIE) [25]:

$$\begin{aligned}&\left[\frac{1}{2}\hat{n}\times\bar{\mathbf{H}} + \hat{n}\times\mathbf{K}(\hat{n}\times\bar{\mathbf{H}}) + \hat{n}\times\mathbf{L}(\mathbf{E}\times\hat{n})\right]\\ &+\hat{n}\times\left[\frac{1}{2}\mathbf{E}\times\hat{n} + \hat{n}\times\mathbf{K}\left(\mathbf{E}\times\hat{n}\right) - \hat{n}\times\mathbf{L}\left(\hat{n}\times\bar{\mathbf{H}}\right)\right]\\ =\ &\hat{n}\times\bar{\mathbf{H}}^{inc}(\mathbf{r}) - \hat{n}\times\hat{n}\times\mathbf{E}^{inc}(\mathbf{r}) \qquad \mathbf{r}\in S\end{aligned} \quad (2)$$

with

$$\mathbf{L}(\mathbf{X}) = jk_0\int_S\left[\mathbf{X}\left(\mathbf{r}'\right)G_0(\mathbf{r},\mathbf{r}') + \frac{1}{k_0^2}\nabla'\cdot\mathbf{X}\left(\mathbf{r}'\right)\nabla G_0(\mathbf{r},\mathbf{r}')\right]ds' \quad (3)$$

$$\mathbf{K}(\mathbf{X}) = \int_S \mathbf{X}(\mathbf{r}')\times\nabla G_0(\mathbf{r},\mathbf{r}')ds' \quad (4)$$

where the singular point $\mathbf{r} = \mathbf{r}'$ in (4) is removed.

According to the non-overlapping domain decomposition method, we decompose the interior FEM domain into N non-overlapping sub-domains and also separate exterior boundary as another sub-domain from interior FEM domain in the same way. These sub-domains are denoted as $V_p(p = 1, 2, \ldots, N, N+1)$ as illustrated by Fig. 1, where the last sub-domain V_{N+1} refers to the exterior boundary surface S. $\Gamma_{j,i}$ is used to represent the inner interface of sub-domain V_i adjacent to V_j, with the corresponding outward unit normal vector being $\hat{n}_i$.

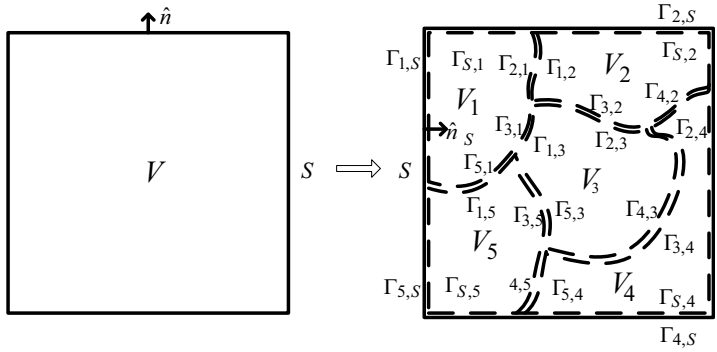

Figure 1. Illustration of domain decomposition.

The field in the ith interior sub-domain satisfies the following differential equation and boundary condition.

$$\begin{aligned} \nabla \times [\mu_{r,i}]^{-1}(\nabla \times \mathbf{E}_i) - k_0^2[\varepsilon_{r,i}]\mathbf{E}_i = 0, \quad &\text{in} \quad V_i \in R^3 \\ \hat{n}_i \times \mathbf{E}_i = 0, \quad &\text{on} \quad \partial V_{PEC,i} \\ \hat{n}_i \times \nabla \times \mathbf{E}_i = 0, \quad &\text{on} \quad \partial V_{PMC,i} \end{aligned} \tag{5}$$

In order to guarantee the field continuity at the sub-domain interfaces and to get a convergent solution, a Robin-type transmission condition is imposed at interfaces as (6).

$$\begin{aligned} &\hat{n}_i \times [\mu_{r,i}]^{-1}\nabla \times \mathbf{E}_i - jk_0\hat{n}_i \times \mathbf{E}_i \times \hat{n}_i \\ &= -\hat{n}_j \times [\mu_{r,j}]^{-1}\nabla \times \mathbf{E}_j - jk_0\hat{n}_j \times \mathbf{E}_j \times \hat{n}_j \quad \text{on} \quad \Gamma_{j,i} \end{aligned} \tag{6}$$

In addition, dual variables, denoted as $\mathbf{J}_i$ and $\mathbf{J}_j$, are imported at the interfaces to decouple the adjacent sub-domains:

$$\begin{aligned} \mathbf{J}_i &= \frac{1}{-jk_0}\left(\hat{n}_i \times [\mu_{r,i}]^{-1}\nabla \times \mathbf{E}_i\right) = \hat{n}_i \times \bar{\mathbf{H}}_i \quad \text{at} \quad \Gamma_{j,i} \\ \mathbf{J}_j &= \frac{1}{-jk_0}\left(\hat{n}_j \times [\mu_{r,j}]^{-1}\nabla \times \mathbf{E}_j\right) = \hat{n}_j \times \bar{\mathbf{H}}_j \quad \text{at} \quad \Gamma_{i,j} \end{aligned} \tag{7}$$

In this way, each sub-domain becomes separated completely and can be solved independently through combination of (5) and (6).

The domain of exterior boundary is formulated by the combined integral Equation (2) and the Robin-type transmission condition (6). The Robin-type transmission condition becomes the link between exterior boundary and interior domain.

The boundary value problem formulated by differential Equations (5) and (6) is solved by finite element method. Firstly, the whole interior domain is meshed by tetrahedral elements. Secondly, the whole

interior domain is decomposed into N sub-domains. The electric field $\mathbf{E}_i$ in the ith sub-domain is expanded with edge-element vector basis function $\mathbf{W}_{m,i}$, and $\mathbf{J}_i$ at the sub-domain interface is expanded with $\hat{n}_i \times \mathbf{W}_{m,\Gamma,i}$, which yields (8) and (9).

$$\mathbf{E}_i = \sum_{m=1}^{M} E_{m,i}\mathbf{W}_{m,i} = \mathbf{W}_i^{\mathrm{T}} \cdot E_i = E_i^{\mathrm{T}} \cdot \mathbf{W}_i \tag{8}$$

$$\begin{aligned}\mathbf{J}_i &= \hat{n}_i \times \bar{\mathbf{H}}_i = \sum_{m=1}^{M_\Gamma} \bar{H}_{m,i}(n_i \times \mathbf{W}_{m,\Gamma,i}) = \bar{H}_i^{\mathrm{T}} \cdot (n_i \times \mathbf{W}_{\Gamma,i}) \\ &= (n_i \times \mathbf{W}_{\Gamma,i})^{\mathrm{T}} \cdot \bar{H}_i \end{aligned} \tag{9}$$

with M and M_Γ are the number of terms that expand $\mathbf{E}_i$ and $\mathbf{J}_i$, respectively.

For any interior sub-domain, by Galerkin's method, (5) and (6) are tested by $\mathbf{W}_i$ and $\hat{n}_i \times \mathbf{W}_{\Gamma,i}$, respectively. Thus, the FEM equation for the ith sub-domain is derived as (10).

$$\begin{bmatrix} \mathbf{A}_{II,i} & \mathbf{A}_{I\Gamma,i} & 0 \\ \mathbf{A}_{I\Gamma,i}^{T} & \mathbf{A}_{\Gamma\Gamma,i} & \mathbf{C}_i \\ 0 & \mathbf{C}_i^{\mathrm{T}} & \mathbf{D_i} \end{bmatrix} \begin{bmatrix} E_{I,i} \\ E_{\Gamma,i} \\ \bar{H}_{\Gamma,i} \end{bmatrix} = \sum_{j \in neighbour(i)} \begin{bmatrix} 0 & 0 & 0 \\ 0 & 0 & 0 \\ 0 & \mathbf{F}_{j,i} & \mathbf{G}_{j,i} \end{bmatrix} \begin{bmatrix} E_{I,j} \\ E_{\Gamma,j} \\ \bar{H}_{\Gamma,j} \end{bmatrix} \tag{10}$$

Here, Γ represents field at the sub-domain interfaces and I represents the field except that at interfaces. The sub-matrices in (10) are as follows.

$$\begin{aligned}\mathbf{A}_i &= \begin{bmatrix} \mathbf{A}_{II,i} & \mathbf{A}_{I\Gamma,i} \\ \mathbf{A}_{I\Gamma,i}^{\mathrm{T}} & \mathbf{A}_{\Gamma\Gamma,i} \end{bmatrix} \\ &= \int_{V_i} \left[(\nabla \times \mathbf{W}_i) \cdot [\mu_{r,i}]^{-1} (\nabla \times \mathbf{W}_i)^{\mathrm{T}} - k_0^2 \mathbf{W}_i \cdot [\varepsilon_{r,i}] \mathbf{W}_i^{\mathrm{T}} \right] dv \end{aligned} \tag{11}$$

$$\mathbf{C}_i = -jk_0 \int_{\Gamma_i} \mathbf{W}_{\Gamma,i} \cdot (\hat{n}_i \times \mathbf{W}_{\Gamma,i})^{\mathrm{T}} ds \tag{12}$$

$$\mathbf{D}_i = -jk_0 \int_{\Gamma_i} (\hat{n}_i \times \mathbf{W}_{\Gamma,i}) \cdot (\hat{n}_i \times \mathbf{W}_{\Gamma,i})^{\mathrm{T}} ds \tag{13}$$

$$\mathbf{F}_{j,i} = -jk_0 \int_{\Gamma_{j,i}} (\hat{n}_i \times \mathbf{W}_{\Gamma,i}) \cdot (\mathbf{W}_{\Gamma,j})^{\mathrm{T}} ds \tag{14}$$

$$\mathbf{G}_{j,i} = jk_0 \int_{\Gamma_{j,i}} (\hat{n}_i \times \mathbf{W}_{\Gamma,i}) \cdot (\hat{n}_j \times \mathbf{W}_{\Gamma,j})^{\mathrm{T}} ds \tag{15}$$

On the boundary of the sub-domain S, we use $\mathbf{W}_s$ to test the Robin-type transmission condition and obtain (16).

$$[\mathbf{K}_S]\, E_S + [\mathbf{M}_S]\, \bar{H}_S = \sum_{j \in neighbour(S)} \left\{ [\mathbf{R}_{j,S}]\, E_{\Gamma,j} + [\mathbf{O}_{j,S}]\, \bar{H}_{\Gamma,j} \right\} \tag{16}$$

where

$$\mathbf{K}_S = -jk_0 \int_S \mathbf{W}_S \cdot (\mathbf{W}_S)^{\mathrm{T}}\, ds \tag{17}$$

$$\mathbf{M}_S = -jk_0 \int_S \mathbf{W}_S \cdot (\hat{n}_S \times \mathbf{W}_S)^{\mathrm{T}}\, ds \tag{18}$$

$$\mathbf{R}_{j,S} = -jk_0 \int_{\Gamma_{j,S}} \mathbf{W}_S \cdot (\mathbf{W}_{\Gamma,j})^{\mathrm{T}} ds \tag{19}$$

$$\mathbf{O}_{j,S} = jk_0 \int_{\Gamma_{j,S}} \mathbf{W}_S \cdot (\hat{n}_j \times \mathbf{W}_{\Gamma,j})^{\mathrm{T}} ds \tag{20}$$

Next, the CFIE on boundary S is discretized by the method of moment (MOM) which yields (21).

$$[\mathbf{P}]\, E_S + [\mathbf{Q}]\, \bar{H}_S = \mathbf{b} \tag{21}$$

The reader is referred to [8] for explicit expressions of the matrices $\mathbf{P}$, $\mathbf{Q}$, and column vector $\mathbf{b}$ in (21).

For the sake of clarity, let

$$X_i = \left[E_{I,i}^{\mathrm{T}}, E_{\Gamma,i}^{\mathrm{T}}, \bar{H}_{\Gamma,i}^{\mathrm{T}}\right]^{\mathrm{T}} \tag{22}$$

$$\tilde{\mathbf{A}}_i = \begin{bmatrix} \mathbf{A}_{II,i} & \mathbf{A}_{I\Gamma,i} & 0 \\ \mathbf{A}_{I\Gamma,i}^{T} & \mathbf{A}_{\Gamma\Gamma,i} & \mathbf{C}_i \\ 0 & \mathbf{C}_i^{\mathrm{T}} & \mathbf{D}_i \end{bmatrix} \tag{23}$$

$$\mathbf{S}_{j,i} = \begin{bmatrix} 0 & 0 & 0 \\ 0 & 0 & 0 \\ 0 & \mathbf{F}_{j,i} & \mathbf{G}_{j,i} \end{bmatrix} \tag{24}$$

Thus, (10) takes the form

$$\tilde{\mathbf{A}}_i X_i = \sum_{j \in neighbour(i)} \mathbf{S}_{j,i} X_j \tag{25}$$

To proceed further, we introduce projection Boolean matrices $\mathbf{B}_{E\bar{H},\Gamma,i}$ and $\mathbf{B}_{\bar{H},\Gamma,i}$ satisfying $\nu_i = \left[E_{\Gamma,i}^{\mathrm{T}}, \bar{H}_{\Gamma,i}^{\mathrm{T}}\right]^{\mathrm{T}} = \mathbf{B}_{E\bar{H},\Gamma,i} X_i$, $\bar{H}_{\Gamma,i} = \mathbf{B}_{\bar{H},\Gamma,i} X_i$, respectively. Then, multiply $\tilde{\mathbf{A}}_i^{-1}$ on both sides of (25) and remove $E_{I,i}$ at the same time. An equation only related with the field at interfaces is obtained as (26).

$$\nu_i = \sum_{j \in neighbour(i)} \mathbf{Z}_i \mathbf{N}_{j,i} \nu_j \tag{26}$$

with

$$\mathbf{Z}_i = \mathbf{B}_{E\bar{H},\Gamma,i} \tilde{\mathbf{A}}_i^{-1} \mathbf{B}_{\bar{H},\Gamma,i}^{\mathrm{T}} \tag{27}$$

$$\mathbf{N}_{j,i} = [\ \mathbf{F}_{j,i} \quad \mathbf{G}_{j,i}\ ] \tag{28}$$

Assemble the interior sub-domains with exterior boundary domain through Equations (16), (21), and (26). The system matrix equation of DDM-FE-BI-MLFMA is derived as (29).

$$\begin{bmatrix} \mathbf{I}_1 & -\mathbf{Z}_1\mathbf{N}_{2,1} & \dots & -\mathbf{Z}_1\mathbf{N}_{3,1} & -\mathbf{Z}_1\mathbf{F}_{S,1} & -\mathbf{Z}_1\mathbf{G}_{S,1} \\ -\mathbf{Z}_2\mathbf{N}_{1,2} & \mathbf{I}_2 & \dots & -\mathbf{Z}_2\mathbf{N}_{3,2} & -\mathbf{Z}_2\mathbf{F}_{S,2} & -\mathbf{Z}_2\mathbf{G}_{S,2} \\ \vdots & \vdots & \ddots & \vdots & \vdots & \vdots \\ -\mathbf{Z}_N\mathbf{N}_{1,N} & -\mathbf{Z}_N\mathbf{N}_{2,N} & \dots & \mathbf{I}_N & -\mathbf{Z}_N\mathbf{F}_{S,N} & -\mathbf{Z}_N\mathbf{G}_{S,N} \\ -\mathbf{K}_S^{-1}\mathbf{N}'_{1,S} & -\mathbf{K}_S^{-1}\mathbf{N}'_{2,S} & \dots & -\mathbf{K}_S^{-1}\mathbf{N}'_{N,S} & \mathbf{I}_{E,S} & \mathbf{K}_S^{-1}\mathbf{M}_S \\ 0 & 0 & \dots & 0 & \mathbf{P} & \mathbf{Q} \end{bmatrix}$$
$$\begin{bmatrix} \nu_1 \\ \nu_2 \\ \vdots \\ \nu_N \\ E_s \\ \bar{H}_s \end{bmatrix} = \begin{bmatrix} 0 \\ 0 \\ 0 \\ 0 \\ 0 \\ \mathbf{b} \end{bmatrix} \tag{29}$$

where $\mathbf{N}'_{j,S} = [\mathbf{R}_{j,S} \quad \mathbf{O}_{j,S}]$.

From (29), it is obvious that the original 3D problem is reduced to an interface problem for the unknown boundary conditions. Because the number of unknowns in each sub-domain is much smaller than that in the whole domain, the memory for solving $\tilde{\mathbf{A}}_i^{-1}$ directly is saved significantly. Equation (29) can be solved using a Krylov subspace method with the aid of MLFMA which speeds up the matrix-vector multiplication of $\mathbf{P}E_{\mathbf{s}}$ and $\mathbf{Q}\bar{H}_s$.

2.2. ABC-SSOR Preconditioner

Although the condition of coefficient matrix of (29) is much better than that of the conventional FE-BI-MLFMA, it is still not well-conditioned, and hence leads to a slow convergence. To further improve the convergence of DDM-FE-BI-MLFMA, a novel efficient preconditioner is constructed below.

[9] proposed an ABC preconditioner and verified its efficiency for accelerating the convergence of the conventional FE-BI-MLFMA by numerical experiments. Referring to it, the proposed method firstly introduces the first-order absorbing boundary condition to approximate the boundary integral equation, and yields a matrix $\bar{\mathbf{P}}$

shown by (30).

$$\bar{\mathbf{P}} = \begin{bmatrix} \mathbf{I}_1 & -\mathbf{Z}_1\mathbf{N}_{2,1} & \dots & -\mathbf{Z}_1\mathbf{N}_{3,1} & -\mathbf{Z}_1\mathbf{F}_{S,1} & -\mathbf{Z}_1\mathbf{G}_{S,1} \\ -\mathbf{Z}_2\mathbf{N}_{1,2} & \mathbf{I}_2 & \dots & -\mathbf{Z}_2\mathbf{N}_{3,2} & -\mathbf{Z}_2\mathbf{F}_{S,2} & -\mathbf{Z}_2\mathbf{G}_{S,2} \\ \vdots & \vdots & \ddots & \vdots & \vdots & \vdots \\ -\mathbf{Z}_N\mathbf{N}_{1,N} & -\mathbf{Z}_N\mathbf{N}_{2,N} & \dots & \mathbf{I}_N & -\mathbf{Z}_N\mathbf{F}_{S,N} & -\mathbf{Z}_N\mathbf{G}_{S,N} \\ -\mathbf{N}'_{1,S} & -\mathbf{N}'_{2,S} & \dots & -\mathbf{N}'_{N,S} & \mathbf{K}_S & \mathbf{M}_S \\ 0 & 0 & \dots & 0 & -\mathbf{M}_S^{\mathrm{T}} & \mathbf{V}_S \end{bmatrix} \tag{30}$$

where $\mathbf{V}_S = -jk_0 \int_S (\hat{n} \times \mathbf{W}_S) \cdot (\hat{n} \times \mathbf{W}_S)^{\mathrm{T}}\, ds$. Note that the last two rows are corresponding to the boundary domain. Similar to the process obtaining (26), we treat these two rows in $\bar{\mathbf{P}}$ and get matrix $\tilde{\mathbf{P}}$.

$$\tilde{\mathbf{P}} = \begin{bmatrix} \mathbf{I}_1 & -\mathbf{Z}_1\mathbf{N}_{2,1} & \dots & -\mathbf{Z}_1\mathbf{N}_{N,1} & -\mathbf{Z}_1\mathbf{N}_{S,1} \\ -\mathbf{Z}_2\mathbf{N}_{1,2} & \mathbf{I}_2 & \dots & -\mathbf{Z}_2\mathbf{N}_{N,2} & -\mathbf{Z}_2\mathbf{N}_{S,2} \\ \vdots & \vdots & \ddots & \vdots & \vdots \\ -\mathbf{Z}_N\mathbf{N}_{1,N} & -\mathbf{Z}_N\mathbf{N}_{2,N} & \dots & \mathbf{I}_N & -\mathbf{Z}_N\mathbf{N}_{S,N} \\ -\mathbf{Z}'_S\mathbf{N}'_{1,S} & -\mathbf{Z}'_S\mathbf{N}'_{2,S} & \dots & -\mathbf{Z}'_S\mathbf{N}'_{N,S} & \mathbf{I}_S \end{bmatrix} \tag{31}$$

where

$$\mathbf{Z}'_s = \begin{bmatrix} \mathbf{K}_S & \mathbf{M}_S \\ -\mathbf{M}_S^{\mathrm{T}} & \mathbf{V}_S \end{bmatrix}^{-1} \mathbf{B}_{E,S}^{\mathrm{T}} \tag{32}$$

with $\mathbf{B}_{E,S}$ is another Boolean matrix which satisfies $E_S = \mathbf{B}_{E,S}[E_S^T \;\; \bar{H}_S^T]^T$.

The form of matrix (31) is suitable for adopting block symmetric successive over relaxation (SSOR) technique [20]. Thus, a novel mixed preconditioner $\tilde{\mathbf{P}}_{\text{ABC-SSOR}}$ (33) for the DDM-FE-BI-MLFMA is constructed. Because it includes absorbing boundary condition, it is referred as ABC-SSOR preconditioner in this paper.

$$\tilde{\mathbf{P}}_{\text{ABC-SSOR}} = \mathbf{L}\mathbf{U},$$

$$\mathbf{L} = \begin{bmatrix} \mathbf{I}_1 & 0 & \dots & 0 & 0 \\ -\mathbf{Z}_2\mathbf{N}_{1,2} & \mathbf{I}_2 & \dots & 0 & 0 \\ \vdots & \vdots & \ddots & \vdots & \vdots \\ -\mathbf{Z}_N\mathbf{N}_{1,N} & -\mathbf{Z}_N\mathbf{N}_{2,N} & \dots & \mathbf{I}_N & 0 \\ -\mathbf{Z}'_S\mathbf{N}'_{1,S} & -\mathbf{Z}'_S\mathbf{N}'_{2,S} & \dots & -\mathbf{Z}'_S\mathbf{N}'_{N,S} & \mathbf{I}_S \end{bmatrix},$$

$$\mathbf{U} = \begin{bmatrix} \mathbf{I}_1 & -\mathbf{Z}_1\mathbf{N}_{2,1} & \dots & -\mathbf{Z}_1\mathbf{N}_{N,1} & -\mathbf{Z}_1\mathbf{N}_{S,1} \\ 0 & \mathbf{I}_2 & \dots & -\mathbf{Z}_2\mathbf{N}_{N,2} & -\mathbf{Z}_2\mathbf{N}_{S,2} \\ \vdots & \vdots & \ddots & \vdots & \vdots \\ 0 & 0 & \dots & \mathbf{I}_N & -\mathbf{Z}_N\mathbf{N}_{S,N} \\ 0 & 0 & \dots & 0 & \mathbf{I}_S \end{bmatrix} \tag{33}$$

Note that $\mathbf{L}$ is the block lower part of $\tilde{\mathbf{P}}_{\text{ABC-SSOR}}$, while $\mathbf{U}$ is its upper part. It is obvious that it is simple to solve the inverse of matrix $\tilde{\mathbf{P}}_{\text{ABC-SSOR}}$. What's more, there is no requirement for extra computer memory.

3. NUMERICAL EXPERIMENTS

To demonstrate the accuracy, efficiency and capability of the presented hybrid method, a series of numerical experiments are performed on a computer server with 2 Intel X5650 2.66 GHz CPUs, 96 GB memory. The GMRES iterative solver is employed to solve (29) with a restart number of 20. The average edge length of tetrahedral mesh is 0.05λ.

Firstly, to verify the accuracy and efficiency of the preconditioned DDM-FE-BI-MLFMA, the BI-static radar cross section (RCS) of a homogenous dielectric sphere and a dielectric cube are calculated by the conventional FE-BI-MLFMA presented in [8], the FE-BI-MLFMA

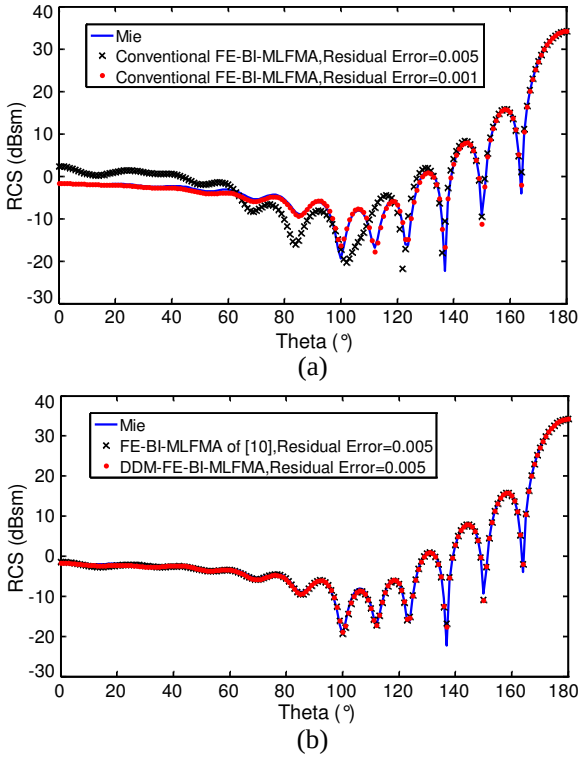

Figure 2. BI-static VV-polarized RCS for the dielectric sphere in the E-plane.

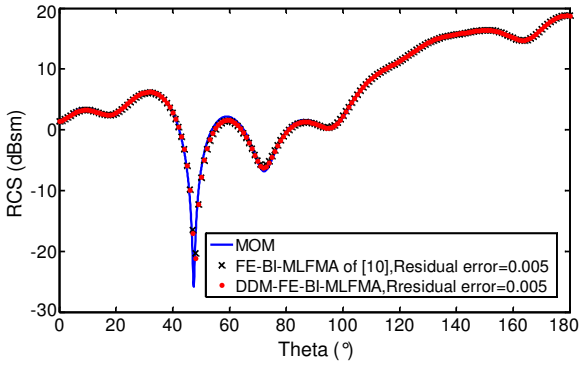

Figure 3. BI-static VV-polarized RCS for the dielectric cube in the E-plane.

of [10], and the preconditioned DDM-FE-BI-MLFMA in this paper, respectively. The sphere constructed with material $\varepsilon_r = 2.0 - 1.0j$ has a diameter of 4λ and is illuminated by plane wave at incidence angle $\theta = 0^\circ, \varphi = 0^\circ$. The number of unknowns in the FEM- and the BI-parts are 607,040 and 19,200, respectively, in totally 50 sub-domains. The cube with $\varepsilon_r = 2.0$ has dimension of $2\lambda \times 2\lambda \times 2\lambda$ and is illuminated by plane wave at incidence angle $\theta = 30^\circ, \varphi = 0^\circ$. The number of unknowns in the FEM- and the BI-parts are 462,520 and 28,800, respectively, in totally 38 sub-domains. The calculated RCS are shown in Fig. 2 and Fig. 3. Fig. 2 and Fig. 3 show that the result of the preconditioned DDM-FE-BI-MLFMA is in good agreement with the Mie series and MOM solutions which verify the high accuracy of the proposed hybrid method. Furthermore, we find the residual error of 0.005 is sufficient for the preconditioned DDM-FE-BI-MLFMA while the conventional FE-BI-MLFMA requires a maximum residual error of 0.001 (Fig. 2). It further confirms that the preconditioned DDM-FE-BI-MLFMA has much smaller condition number than the conventional FE-BI-MLFMA. Table 1 lists the main computational information of the different methods. Compared with the conventional FE-BI-MLFMA, the preconditioned DDM-FE-BI-MLFMA method improves the convergence significantly. Even though the preconditioned DDM-FE-BI-MLFMA needs more iteration number than the FE-BI-MLFMA of [10], it can save computer memory effectively. It can be seen that the FE-BI-MLFMA of [10] consumes more memory than the conventional FE-BI-MLFMA of [8]. The reason is that the required memory in the conventional FE-BI-MLFMA only needs to store sparse matrices [26], whereas that the FE-BI-MLFMA of [10] requires large memory during the inverse of the FEM sparse matrix solved by a sparse direct solver based on the multifrontal approach [27]. Because the preconditioned

DDM-FE-BI-MLFMA decomposes the large FEM sparse matrix into several small sparse matrices and solve the inverse of these small matrices directly, it consumes much less memory than the FE-BI-MLFMA of [10].

To investigate the numerical scalability of the DDM-FE-BI-MLFMA and the efficiency of the ABC-SSOR preconditioner for the DDM-FE-BI-MLFMA, scattering by different homogenous dielectric

Table 1. Computational information of the different methods for two numerical simulations.

Obects	Iteration Number (residual error = 0.005)			Computational memory (GB)		
	[8]	[10]	This paper	[8]	[10]	This paper
Sphere	3295	14	32	0.6	13.15	3.17
Cube	> 10000	77	153	0.9	8.74	2.88
Obects	Total CPU time (s) (residual error = 0.005)					
	[8]	[10]	This paper			
Sphere	1622	359	146			
Cube	> 5000	481	432			

Table 2. Computational information for different objects.

Size	Unknowns		Number of sub-domains
	FEM	BI	
1λ	59,660	7,200	5
2λ	462,520	28,800	38
3λ	1,544,580	64,800	129
4λ	3,641,840	115,200	307
5λ	7,090,300	180,000	600

Size	$\varepsilon_r = 2.0$ Iteration Number		$\varepsilon_r = 2.0 - j$ Iteration Number	
	Without ABC-SSOR	With ABC-SSOR	Without ABC-SSOR	With ABC-SSOR
1λ	141	61	54	27
2λ	404	136	65	32
3λ	659	210	70	34
4λ	862	284	75	36
5λ	1083	364	78	37

cubes under the incident plane wave of $\theta = 0^{\circ}, \varphi = 0^{\circ}$ are calculated. The length of cube is changed from 1λ to 5λ at 1λ step. Two types of objects are investigated. One is lossless dielectric material with $\varepsilon_r = 2.0$ and the other is lossy dielectric material with $\varepsilon_r = 2.0 - j$. Experiments are performed by the DDM-FE-BI-MLFMA without and with ABC-SSOR preconditioner, respectively and the residual error is set to 0.005. Detailed computational information is listed in Table 2.

It can be seen from Table 2 that the iteration number of both without and with preconditioner increases fairly slowly with the enlargement of the lossy cube. This indicates the DDM-FE-BI-MLFMA has a good scalability for lossy dielectric objects. However, the scalability is reduced considerably for lossless dielectric objects. On the other hand, it is obvious that the ABC-SSOR preconditioner can effectively improve the convergence of the DDM-FE-BI-MLFMA treating lossless dielectric objects compared with that without preconditioner.

Finally, two numerical experiments are carried out to demonstrate the capability of the preconditioned DDM-FE-BI-MLFMA for 3D electrically large objects. One is a homogeneous dielectric sphere with diameter of 10λ, and $\varepsilon_r = 3.0 - j$. The other one is a two layers coated sphere with diameter of 20λ. The thickness of each coating layer is 0.05λ and relative permittivity is $3.0 - j$ and $1.0 - j$ from inner to outer. They are illuminated by plane wave at incident angle $\theta = 0°, \varphi = 0°$. The residual error is set to 0.005 in all simulations. The obtained BI-static RCS are plotted in Fig. 4 and Fig. 5 and detailed computational information is listed in Table 3. These two experiments demonstrate that the preconditioned DDM-FE-BI-MLFMA is a powerful tool for 3D electrically large and complex objects.

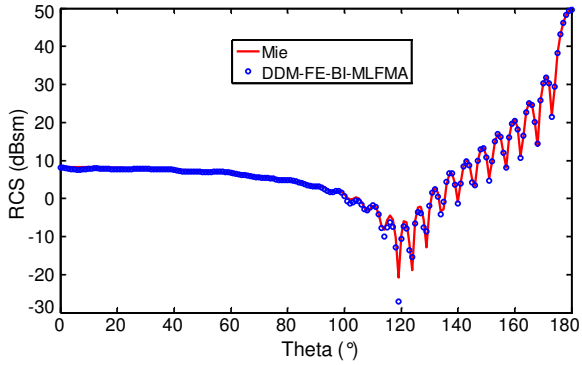

Figure 4. BI-static VV-polarized RCS for the homogeneous dielectric sphere in the E-plane.

Table 3. Computational information for different objects.

Objects	Number of Unknowns		Number of sub-domains
	FEM	BI	
Dielectric Sphere	9,393,600	120,000	800
Coated Sphere	2,720,004	480,000	192
Objects	Memory (GB)	Iteration Number	Time (min)
Dielectric Sphere	71.81	59	49
Coated Sphere	13.15	122	61

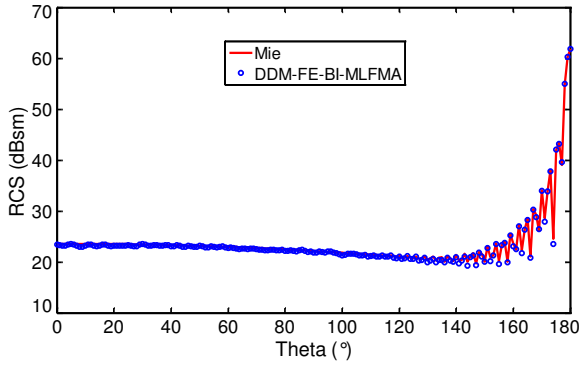

Figure 5. BI-static VV-polarized RCS for the coated sphere in the E-plane.

4. CONCLUSIONS

FE-BI-MLFMA combined with a non-overlapping domain decomposition method is presented in this paper. It employs Robin-type transmission condition to not only decompose interior FEM domain into several sub-domains but also separate exterior boundary surface from interior FEM domain. By a series of mathematic transformations, the three-dimensional problem is transformed into a problem related with sub-domain interfaces. Furthermore, a novel ABC-SSOR preconditioner is constructed to improve the convergence of DDM-FE-BI-MLFMA. Numerical experiments are performed to demonstrate the capability of this new hybrid method. Compared with the con-

ventional FE-BI-MLFMA, the preconditioned DDM-FE-BI-MLFMA can speed up the iterative convergence significantly. What's more, it doesn't consume memory strongly. Numerical results show that the proposed method demonstrates good scalability for lossy dielectric objects. However, its scalability reduces for lossless dielectric objects. The proposed novel ABC-SSOR preconditioner can further improve the convergence of the DDM-FE-BI-MLFMA, especially in treating the slow convergence phenomenon of lossless medium. High capability of the preconditioned DDM-FE-BI-MLFMA is also demonstrated by numerical experiments.

ACKNOWLEDGMENT

This work was supported by the National Basic Research Program (973) under Grant 2012CB720702.

REFERENCES

1. Yuan, X., "Three-dimensional electromagnetic scattering from inhomogeneous objects by the hybrid moment and finite element method," *IEEE Trans. Microwave Theory Tech.*, Vol. 38, 1053–1058, Aug. 1990.
2. Jin, J. M. and J. L. Volakis, "A hybrid finite element method for scattering and radiation by microstrip patch antennas and arrays residing in a cavity," *IEEE Trans. Antennas Propagat.*, Vol. 39, 1598–1604, Nov. 1991.
3. Angelini, J. J., C. Soize, and P. Soudais, "Hybrid numerical method for harmonic 3-D Maxwell equations: Scattering by a mixed conducting and inhomogeneous anisotropic dielectric medium," *IEEE Trans. Antennas Propagat.*, Vol. 41, 66–76, May 1993.
4. Eibert, T. and V. Hansen, "Calculation of unbounded field problems in free space by a 3-D FEM/BEM-hybrid approach," *Journal of Electromagnetic Waves and Applications*, Vol. 10, No. 1, 61–77, Apr. 1996.
5. Shao, H., J. Hu, Z.-P. Nie, G. Han, and S. He, "Hybrid tangential equivalence principle algorithm with MLFMA for analysis of array structures," *Progress In Electromagnetics Research*, Vol. 113, 127–141, 2011.
6. Ergül, Ö., "Parallel implementation of MLFMA for homogeneous objects with various material properties," *Progress In Electromagnetics Research*, Vol. 121, 505–520, 2011.

7. Pan, X.-M., L. Cai, and X.-Q. Sheng, "An efficient high order multilevel fast multipole algorithm for electromagnetic scattering analysis," *Progress In Electromagnetics Research*, Vol. 126, 85–100, 2012.
8. Sheng, X. Q., J. M. Song, C. C. Lu, and W. C. Chew, "On the formulation of hybrid finite-element and boundary-integral method for 3D scattering," *IEEE Trans. Antennas Propagat.*, Vol. 46, 303–311, Mar. 1998.
9. Liu, J. and J. M. Jin, "A highly effective preconditioner for solving the finite element-boundary integral matrix equation for 3-D scattering," *IEEE Trans. Antennas Propagat.*, Vol. 50, 1212–1221, Sep. 2002.
10. Sheng, X. Q. and E. K. N. Yung, "Implementation and experiments of a hybrid algorithm of the MLFMA-Enhanced FE-BI method for open-region inhomogeneous electromagnetic problems," *IEEE Trans. Antennas Propagat.*, Vol. 50, 163–167, Feb. 2002.
11. Peng, Z., X. Q. Sheng, and F. Yin, "An efficient twofold iterative algorithm of FE-BI-MLFMA using multilevel inverse-based ILU preconditioning," *Progress In Electromagnetics Research*, Vol. 93, 369–384, 2009.
12. Farhart, C. and F. X. Roux, "A method of finite element tearing and interconnecting and its parallel solution algorithm," *Int. J. Numer. Method Eng.*, Vol. 32, 1205–1227, 1991.
13. Stupfel, B., "A fast-domain decomposition method for the solution of electromagnetic scattering by large objects," *IEEE Trans. Antennas Propagat.*, Vol. 44, 1375–1385, Oct. 1996.
14. Wolfe, C. T., U. Navsariwala, and S. D. Gedney, "An efficient implementation of the finite-element time-domain algorithm on parallel computers using finite-element tearing and interconnecting algorithm," *Microwave and Optical Technology Letters*, Vol. 16, No. 4, Nov. 1997.
15. Wolfe, C. T., U. Navsariwala, and S. D. Gedney, "A parallel finite-element tearing and interconnecting algorithm for solution of the vectorwave equation with PML absorbing medium," *IEEE Trans. Antennas Propagat.*, Vol. 48, 278–284, Feb. 2000.
16. Stupfel, B. and M. Mognot, "A domain decomposition method for the vector wave equation," *IEEE Trans. Antennas Propagat.*, Vol. 48, 653–660, May 2000.
17. Vouvakis, M. N. and J.-F. Lee, "A fast non-conforming DP-FETI domain decomposition method for the solution of large EM problems," *Proc. Antennas Propag. Soc. Int. Symp.*, Vol. 1, 623–

626, Jun. 2004.

18. Lee, S.-C., M. N. Vouvakis, and J.-F. Lee, "A non-overlapping domain decomposition method with non-matching grids for modeling large finite antenna arrays," *J. Comput. Phys.*, Vol. 203, 1–21, Feb. 2005.
19. Vouvakis, M. N., Z. Cendes, and J.-F. Lee, "A FEM domain decomposition method for photonic and electromagnetic band gap structures," *IEEE Trans. Antennas Propagat.*, Vol. 54, 721–733, Feb. 2006.
20. Lü, Z. Q., X. An, and W. Hong, "A fast domain decomposition method for solving three-dimensional large-scale electromagnetic problems," *IEEE Trans. Antennas Propagat.*, Vol. 56, 2200–2210, Aug. 2008.
21. Li, Y. J. and J.-M. Jin, "A vector dual-primal finite element tearing and interconnecting method for solving 3-D large-scale electromagnetic problems," *IEEE Trans. Antennas Propagat.*, Vol. 54, 3000–3009, Oct. 2006.
22. Li, Y. J. and J. M. Jin, "A new dual-primal domain decomposition approach for finite element simulation of 3-D large-scale electromagnetic problems," *IEEE Trans. Antennas Propagat.*, Vol. 55, 2803–2810, Oct. 2007.
23. Cui, Z. W., Y. Han, C. Y. Li, and W. J. Zhao, "Efficient analysis of scattering from multiple 3-D cavities by means of a FE-BI-DDM method," *Progress In Electromagnetics Research,* Vol. 116, 425–439, 2011.
24. Yang, M. L. and X. Q. Sheng, "On the finite element tearing and interconnecting method for scattering by large 3D inhomogeneous targets," *International Journal of Antennas and Propagat.*, Vol. 2012, 1–6, 2012.
25. Jin, J. M., *The Finite Element Method in Electromagnetics*, 2nd Edition, Wiley, New York, 2002.
26. Dziekonski, A., A. Lamecki, and M. Mrozowski, "A memory efficient and fast sparse matrix vector product on a GPU," *Progress In Electromagnetics Research*, Vol. 116, 49–63, 2011.
27. Amestoy, P. R., I. S. Duff, J.-Y. L'Excellent, and J. Koster, "A full asynchronous multifrontal solver using distributed dynamic scheduling," *SIAM J. Matrix Anal. Appl.*, Vol. 23, No. 1, 15–41, Jan. 2001.